ISSN 0095-4527, Cytology and Genetics, 2022, Vol. 56, No. 2, pp. 125–138. © Allerton Press, Inc., 2022.
Ukrainian Text © The Author(s), 2022, published in Tsitologiya i Genetika, 2022, Vol. 56, No. 2, pp. 21–37.

Effect of Implantation of a Fibrin Matrix Associated with Neonatal Brain Cells on the Course of an Experimental Spinal Cord Injury

V. V. Medvediev[a], *, N. P. Oleksenko[b], **, L. D. Pichkur[b], *, S. A. Verbovska[b], ****, S. I. Savosko[a], *****, N. G. Draguntsova[b], ******, Yu. A. Lontkovskiy[c], *******, V. V. Vaslovych[b], ********, and V. I. Tsymbalyuk[d], **********

[a] *Bogomolets National Medical University, Kyiv, 01601 Ukraine*
[b] *Romodanov Institute of Neurosurgery, National Academy of Medical Sciences of Ukraine, Kyiv, 04050 Ukraine*
[c] *Kam'yanets-Podil's'ka Municipal Hospital, Kam'yanets-Podil's'kyi, Khmel'nyts'k oblast, 32301 Ukraine*
[d] *National Academy of Medical Sciences of Ukraine, Kyiv, 04050 Ukraine*
**e-mail: vavo2010@gmail.com*
***e-mail: noleksenko@gmail.com*
****e-mail: l.pichkur@neuro.kiev.ua*
*****e-mail: verbovskaya-svetlana@ukr.net*
******e-mail: savosko_s@ukr.net*
*******e-mail: natalya.exlab@gmail.com*
********e-mail: yulont@ukr.net*
*********e-mail: greycat312@gmail.com*
*********e-mail: tsymb777@gmail.com*

Received June 25, 2021; revised September 21, 2021; accepted March 18, 2022

Abstract—The effect of immediate implantation of a fibrin matrix associated with allogeneic neonatal rat brain cells on their motor function recovery after a spinal cord injury (SCI) was studied. The cohorts of animals selected for the study were represented by white adult outbred rats (approximately 260 g each, 4 or 5 months old). The SCI simulation was based on a left-side hemisection of the spinal cord at the level of approximately T_{13}–L_1 segments. The rehabilitation treatment included immediate transplantation of a human fibrin matrix associated with neonatal rat brain cells (NBCs) ($n = 9$) into the injury area. The reference groups were represented by animals with isolated traumatic (Tr) SCIs ($n = 7$) and those with implantation of a human acellular fibrin (Fb) matrix ($n = 6$) into the injury area. The motor activity was assessed in the paretic hindlimb on the Basso, Beattie, and Bresnahan (BBB) scale; spasticity was evaluated on the Ashworth scale; and the pathohistological examination of longitudinal spinal cord sections sampled in the remote posttraumatic period was performed using the silver impregnation staining method. The fibrin matrix promotes viability, growth, and differentiation in the incorporated neonatal rat brain cells. Starting from the second or third week after the implantation into the injury epicenter, the motor function in the paretic limb corresponded to approximately 11 points in the Fb and NBC groups and to approximately six points in the Tr group on the BBB locomotor scale. No significant differences in the locomotor function of the paretic limb were recorded throughout the entire experiment between the NBC and Fb groups nor between the Fb and Tr groups. Significant differences between the NBC and Tr groups were recorded from the second, fourth, and eighth week, as well as the third and fifth months, post injury. A significant prevalence in the level of spasticity in the Tr group over the NBC and Fb groups was recorded, respectively, from the sixth and the seventh week after the injury. An immediate implantation of the fibrin matrix in complex with allogeneic neonatal brain cells or without the latter causes a significant positive effect on the motor function recovery after a lacerative SCI.

Keywords: neurotransplantation, fibrin matrix, spinal cord injury, neonatal brain cells, locomotor function recovery, spasticity

DOI: 10.3103/S0095452722020086

INTRODUCTION

A spinal cord injury (SCI) is an invalidating lesion of the nervous system, which substantially degrades the quality of life for the injured and shortens their lifespan (DeVivo, 2012; Prettz et al., 2016). According to the 2016 Global Burden of Disease estimate (GBD 2016 Traumatic Brain Injury and Spinal Cord Injury Collaborators, 2019), the global morbidity due to SCIs constituted approximately 1 million incidences,

involving approximately 27 millions people. SCIs are much more prevalent among middle-aged men (Singh et al., 2014), while a half of all cases are severe with lifelong invalidation (DeVivo, 2012). Apart from losses in motor function and sensitivity below the injury level, SCI is characterized by dysfunction in the pelvic organs (Hamid et al., 2018), spasticity syndrome (Holtz et al., 2016), chronic pain (Finnerup et al., 2014), as well as cognitive (Sachdeva et al., 2918) and affective (Wan et al., 2020) disorders, which all dramatically increase the treatment and care costs for patients with spinal cord injuries (Oliveri et al., 2014). The underlying causes of the above-listed symptoms include the death of neurons and nerve fibers in the SCI area, first of all, the brain long descending axonal projections providing the self-innervation of motor and spinal cord autonomic centers. Repairing these projections is one of the main tasks of neural tissue engineering (Liu et al., 2018; Wang et al., 2018; Liu et al., 2019; Zhang et al., 2019; Cizkova et al., 2020; Shah et al., 2020). The alternative approach based on grafting the lost motor function, using so called exoskeletons, is now also being successfully developing (Shah et al., 2020; Dijkers et al., 2020), but its application may prove to be possible only in the case of a certain number of long descending axonal projections being preserved in the brain. Therefore, the development of neuroengineering techniques for repairing these projections remains a highly important task.

The most common neural-engineering intervention in SCIs is cell-based transplantation (Muheremu et al., 2016); Lin et al., 2018; Liu et al., 2018), while the method to increase its efficacy is based on the association of cells with polymer matrices or tissue constructions (Liu et al., 2018; Wang et al., 2018; Liu et al., 2019; Zhang et al., 2019). Fibrin gel represents the most promising natural scaffold characterized by accessibility, autogenicity (Tatullo et al., 2012), nontoxicity, susceptibility to biodegradation, 3D structurality, cyto-attractiveness, and saturation with a group of important regulatory and metabolic factors (Amable et al., 2013; Hotwani et al., 2014; Yao et al., 2016). All this promotes the survival and integration of transplanted cells, activating the growth of nerve fibers (Muller et al., 1984) and, thus, potentiates the repair process (Litvinov et al., 2005; Cargnello et al., 2011; Robinson et al., 2017; Lu et al., 2014). These fibrin matrix abilities are usable for the individual combination of maintenance factors and the differentiation of transplanted cells (Carriel et al., 2013; Carriel et al., 2015; Schuh et al., 2015).

This work aimed to study the effect of transplanting allogeneic neonatal rat brain cells in a complex with a human fibrin matrix on the process of recovery after the lateral hemisection of the rat spinal cord in the lower thoracic–upper lumbar spine, using some standard methods for the assessment of motor function in the paretic hindlimb and the standard pathohistological examination.

MATERIALS AND METHODS

Experimental animals. The experiments were performed in 22 white outbred male rats (age of 4 or 5 months) weighing approximately 260 *g* and grown in standard conditions of the Romodanov Neurosurgery Institute Vivarium, National Academy of Medical Sciences of Ukraine (NAMS). The animals were divided into three experimental groups (the number of animals was estimated, excluding those within the below specified exclusion criteria): the traumatic (Tr) group with spinal cord injury ($n = 7$); the Fb group with spinal cord injury + implantation of a fibrin matrix fragment into the injury epicenter ($n = 6$); and the NBC group with spinal cord injury + implantation of a fibrin matrix fragment associated with neonatal brain cells (NBC) into the injury epicenter ($n = 9$).

Obtaining the fibrin matrix. The fibrin matrix was obtained from the adult human platelets-rich plasma (Tatullo et al., 2012) without clinical signs of acute pathology. The polymerization duration was 2–3 min at room temperature. Until the moment of implantation, the prepared fibrin hydrogel was kept in an isotonic sodium chloride solution at room temperature for 3–4 h maximum.

Isolation of neonatal rat brain cells. Living immature rat brain cells were obtained on day 2 after their birth. Immediately after decapitation in sterile conditions, craniotomy was performed, the brain in block with the cerebellum was removed, separated from its films ad oculus, transferred to Hanks solution (Biowest, France), homogenized via multiple pipetting, centrifuged at 1200*g* for 10 min, and the precipitate was further resuspended in the human platelets-rich plasma prepared from an analogous donor for polymerization. The total amount and the content of living cells were calculated in a hemocytometer after staining the specimens with 0.2% trypan blue solution (Jenssen Chemica, Belgium). The final cell concentration reached approximately 1×10^6 per mL with at least 70% of living cells. Upon resuspension, fibrin polymerization was initiated (described above) to obtain the material ready for transplantation.

The properties of cells associated with the fibrin matrix were investigated during a 2-week culturing in the Eagle Medium (Biowest, France) with addition of a 10% fetal calf serum without any modification (Biowest, France) at a 5% CO_2 concentration and at 37°C. The medium was replaced every 3–4 days. The living culture was observed and photographed using an inverted light microscope (Nicon, Japan).

SCI modelling. SCI was modelled under general anesthesia induced by intra-abdominal introduction of a cocktail of xylazine (Biowet, Poland; approximately 15 mg/kg) and ketamine (PATPharmac, Ukraine, approximately 70 mg/kg) in moderate aseptic conditions. As in the previous studies (Kopach et al., 2017), the injury area in a deeply anesthetized animal was identified by palpating the caudal end of the animal's

thorax at the place of its fixation to the backbone. In view of the theoretically higher instability of the rest *costae fluctuantes* pairs present in rodents (Ozkan, 2007; Olude et al., 2013), the injury modelling area had to be localized approximately, probably, at the level of T_{11}–T_{12} vertebrae and without the additional use of microsurgical or X-ray visualization techniques. According to the skeletotopic data (Gilerovich et al., 2008; Moonen et al., 2016), the identified region corresponded to the spinal cord T_{13}–L_1 segments. After the linear incision of the roughly shaved and antiseptically-treated skin at the level of approximately T_9–L_1 vertebrae and skeletonizing the posterior surface of the backbone, the chosen interarch space was perforated with a blunted steel rod, and a laminectomy, limited on the right, was performed with curved mosquito forceps. The state of *dura mater spinalis* within the bone window was not determined and the spinal cord was not separated from the adjacent nerve stems before the SCI modelling. The preciseness of the medial incision line was ensured by the preliminary open-end paramedian dorsoventral puncture of the spinal cord with an insulin syringe needle. One of the ophthalmic tips was introduced into the formed canal while the other one embraced the left half of the spinal cord width with nerve endings and incised them repeatedly. The completeness of hemisection was ensured by ophthalmic forceps with a curved rib. With spontaneous cessation of bleeding in the Fb and NBC animals, the spinal cord injury cavity was filled with a preliminarily prepared fibrin matrix. The bone window to the vertebral canal was covered with a subcutaneous connective tissue fragment, the soft tissues and skin were sutured with two rows of knot stitches, and the injury area was treated with a povidone-iodine solution (EGIS, Hungary). A bicylline-5 solution (PAT Kyivmedpreparat) was subcutaneously administered into the posterior cervical region at a dose of approximately 0.55 million units per kg of live weight. A dexamethasone solution was intra-abdominally injected at a dose of approximately 4 mg/kg of live weight as an anti-inflammatory and antiedematous therapy (KRKA, Slovenia). Rats were further accommodated in plastic cages with horizontal lattices at a density of several animals per cage.

Analysis of the function and spasticity indicators. The indicator of the function (IF) in the hindlimb ipsilateral to the injury area was assessed on the Basso-Beattie-Bresnahan (BBB) scale (Basso et al., 1995) with our own technical modifications. In rare cases of deviation in the IF level within the problematic scale interval (between the scores of 16 and 17 points) (Basso et al., 1995), our own differential test was used. The indicator of spasticity (IS) in the spastic hindlimb ipsilateral to the injury area was assessed at the level of the ankle joint (*articulatio talocruralis* on the adapted Ashworth scale (Dong et al., 2005) with our own technical modifications. Spasticity with mild paresis was identified according to the following original criteria: (1) trembling felt more in the paretic hindlimb than in the contralateral one when stretched aside; (2) hypermetric overextension of the paretic hindlimb during the postural counteraction against the sharp traction of the animal over the horizontal surface for its tail. Due to the presence of even one criterion, the IS was assessed at the level of 0.5 points. All investigations of IF and IS were performed by the same experimenter conventionally blinded concerning the individual signs of animals operated by this experimenter and involved in this experiment and, usually, concerning the previous individual locomotion and spasticity testing results. In all cases, the IF and IS values immediately after the injury modelling were accepted as conventionally equal to zero (the spinal shock condition), and the first IF and IS values were determined 1 week after the surgery due to ethical limitations. When there was no confidence in the correctness of the IF and IS integer value in a given animal, the indicator meaning was halved.

To detail the recovery dynamics, we determined the absolute per week IF growth (points per week, points/wk.) using the following equation:

$$\{V_{\mathrm{IF}}\}_n = \frac{\mathrm{IF}_n - \mathrm{IF}_{n-1}}{k},$$

where n was the number of observations and k was the number of weeks within a given time interval.

The absolute per week IS growth was estimated similarly.

Exclusion criteria. The above indicated number of animals for each experimental group exclude animals demonstrating a stable locomotor function deficiency in the contralateral hindlimb (less than or equal to 14 points of BBB were recorded in two animals from the Tr group and three animals from the Fb group with the IF values in the contralateral hindlimb reaching 8, 8, 8, 9, and 11 points of BBB, respectively) as well as signs of self-abusive behavior (one animal from the Fb group) or uncharacteristic neurological disorders of unclear genesis (one animal from the NBC group). The presence of ipsilateral paresis in the abdominal wall muscles or peripheral paresis in the hindlimb muscles, i.e., either too rostralized or caudalized SCI modelling performance, was not specifically studied.

Result representation specificities. The IF and IS monitoring results were represented using the following standardized time scale: on a weekly basis, during the first 2 months (from 1 to 8 weeks), and on a monthly basis, 3, 4, and 5 months post injury. When the observation results were recorded on a weekly basis, the minimum time unit was 7 days, but this unit was termed by the interval between the same dates of two adjacent months with monthly observations. Among very rare cases of reproducing individual IF and IS values, only one case within the compared analytical period (until the fifth month of observation, inclusively) occurred within 4 weeks after injury in NBC and Fb groups, when the individual IF and IS

values were reproduced through interpolation as the mean arithmetic of values at two adjacent observation points. Asymptotic intergroup differences in the testing terms were identified within 1 and 2 weeks, as well as within three months, after injury (14–29% of the corresponding term value under the standardized result representation time schedule; as to other terms, the difference did not exceed 10%). Thus, it is important to note that deviations from the stable significant straightforward dynamics were absent in all experimental groups after the first month of observation.

Pathomorphological investigations. Biomaterials for pathomorphological investigations were obtained during the remote postinjury period (approximately 7 months postinjury in the Tr group and approximately 9 months postinjury in the Fb and NBC groups). Considering that the remote or the late-stage SCI period starting from the sixth posttraumatic month and continuing into the entire subsequent period of an animal's life (Jeong et al., 2021) is characterized by the absence of essential changes in neurological deficiency (Burns et al., 2017), a 2-month interval within this period is insufficient for manifesting a significant dynamics in the functional and morphological changes. In addition, this temporal difference in sampling biomaterials should be considered insufficient for such a functionally significant morphological feature in the region of posttraumatic organization as the presence (not the quantitative indicators) of nerve fibers in it. Immediately after euthanasia of animals by overdosing the above-mentioned narcotic drugs, the vertebral column region containing the injury area was separated and placed in a neutral 10% formalin solution. After several weeks, the spinal cord within the injury area was isolated using a micropreparation technique. Longitudinal 15-μm-thick spinal cord sections obtained on a microtome cryostat (MK-25, SRSR) were stained using the silver impregnation method (Kolomiytsev et al., 1982). With this purpose, the sections were rinsed in succession in an acid-alcohol formalin solution, pyridine, a 30% silver nitrate solution, and an ammoniacal silver solution, and investigated on an Axiophot microscope (Opton, Germany) with a Canon 600 digital camera (Canon Inc., Taiwan), computer-based CAI01ABH analyzer (Selmi, Ukraine) using the Kappa Opto-Electronics GmbH software (Germany) and an object-micrometer.

Statistical investigations. The comparative statistical analysis of the IF and IS, V_{IF} and V_{IS} values in all three groups was conducted until the fifth month inclusively, using the Statistica 10.0 PC software and the Mann–Whitney U-Test, the Wilcoxon Matched Pairs, and the Spearman Rank Order Correlations Tests. The mean values were represented as $M \pm SE$, where M indicated the mean value and SE meant the standard error of the mean value. In all cases, the study results below 0.05 were recognized as statistically significant (at $p < 0.05$).

RESULTS

In vitro study of the fibrin matrix–nerve cells complex. During the first 3 days of culturing the neonatal rat brain cells associated with fibrin, the experimenters were observing active cell migration to the outer matrix as well as the exit of cells beyond its limits, the axonal network formation, and the establishment of spatial intercellular contacts (Figs. 1a, 1b). On days 7 to 10 of culturing, a confluent cell layer characterized by a polymorphic morphology with processes of different sizes and types of branching was observed near the matrix lobules (Figs. 1c, 1d). Analogous types of cells were also observed in the suspension culture, but they did not form any growth areas and were randomly spread over the field of vision (Figs. 1f, 1g). For the same observation period, cells in the matrix inner areas formed a network of processes and neurite-glial fibers straightened towards the outside and established spatial contacts (Fig. 1h). By the end of the second week of culturing, a partial lysis of the fibrin matrix was recorded, but its formed multicellular 3D structurality was preserved (Fig. 1d). This confirmed that viability and the characteristic morphology of the incorporated neonatal brain cells were preserved.

Effect of fibrin and its complex with neonatal rat brain cells on the functional indicators in rats. Investigations of IF in animals with a simulated injury and the implanted fibrin in complex with cells have shown that the IF of the paretic hindlimb in the Tr group ($n = 7$) was equal to 4.1 ± 2.0 points of BBB from the first week after the surgery, increased up to 6.8 ± 1.4 points of BBB (Fig. 2) within the next 2 weeks, and was especially significantly during the third week ($p = 0.046$, as compared to the value by the end of the first week of observation; as estimated by the Wilcoxon Matched Pairs Test). In the subsequent 2 weeks, the IF values varied and reached the actual maximum of 7.7 ± 1.3 points of BBB by the end of the fifth week ($p < 0.05$, as compared to the first, second, and the fourth week of observation; by the Wilcoxon Matched Pairs Test). Substantial changes, as compared to the values in the first 2 weeks of observation, were also recorded during the next three observation terms ($p < 0.05$, as compared between the values of the sixth and the first week of observation, between the seventh and second week, and the eighth and the first one; by the Wilcoxon Matched Pairs Test). No significant changes in the IF were recorded after the fifth week and until the end of observation ($p < 0.05$; by the Wilcoxon Matched Pairs Test). The group IF value was equal to 5.9 ± 1.6 points of BBB at the end of the fifth month (Fig. 2), reaching 6.0 ± 1.7 points of BBB by the end of the seventh month.

The V_{IF} in the Tr group was equal to 4.1 ± 2.0 points/wk. during the first week of observation, falling to its minimum by the end of the first month of observation (-1.3 ± 0.6 points/wk.; $p < 0.05$, as compared to the first week; by Wilcoxon Matched Pairs

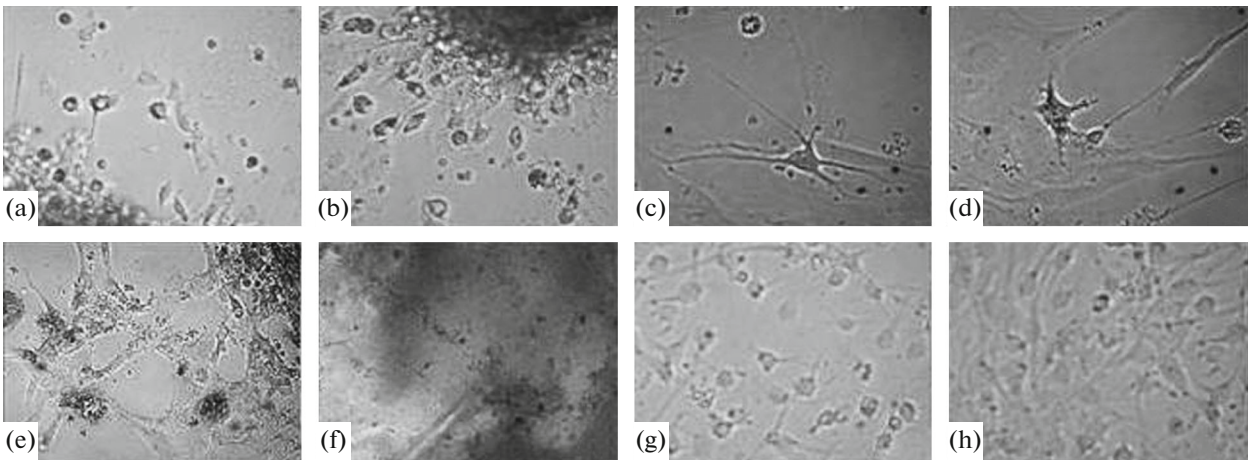

Fig. 1. Rat brain nerve cell culture incorporated into the fibrin matrix. (a, b) On day 3 of culturing, the removal of the cells from the matrix and the growth area formation around it, a living unstained preparation, magnified ×200; (c, d) on days 5 and 7 of culturing, polymorphic nerve cells in the growth area around the matrix, development of intercellular connections, a living unstained preparation, magnified ×200; (e) on day 14 of culturing, partial lysis of the matrix and its replacement by a 3D structure of nerve cells, a living unstained preparation, magnified ×100; (f) on day 7 of culturing, the formation of a cellular lattice in the inner area of the matrix, a living unstained preparation, magnified ×100; (g, h) the rat brain nerve cell suspension culture on days 10 and 14 of culturing, a living unstained preparation, magnified ×200.

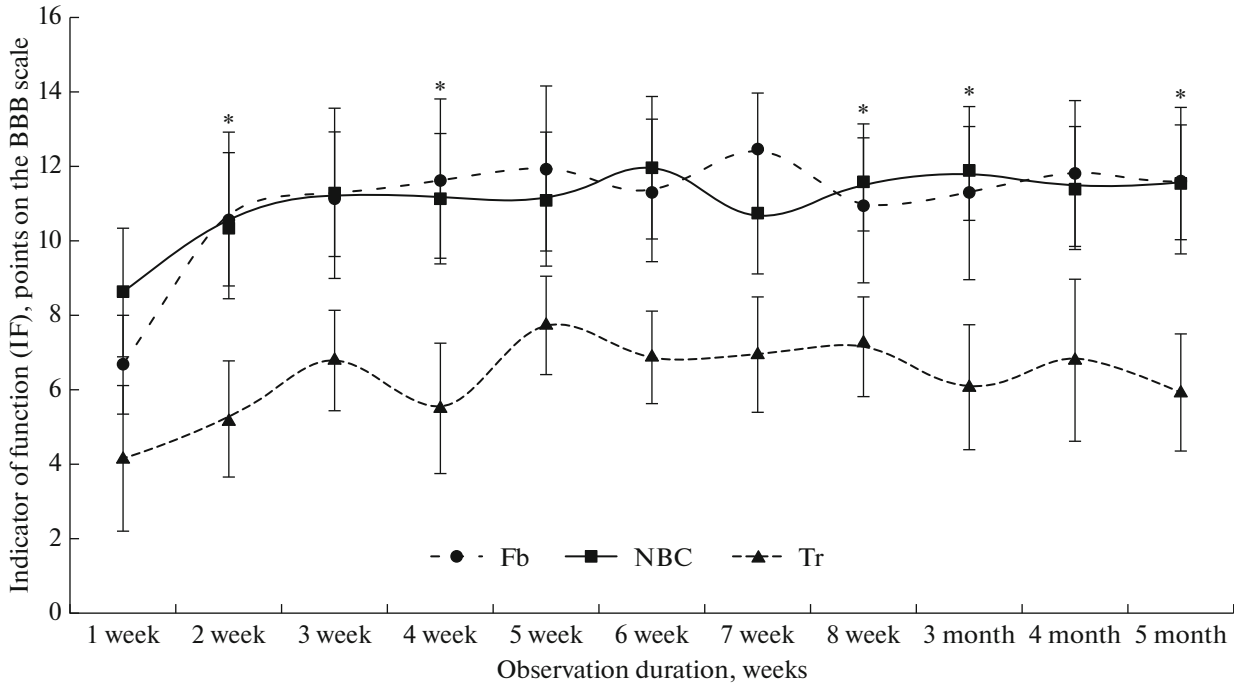

Fig. 2. Dynamics of the indicator of function (IF) in the paretic hindlimb of animals from the experimental groups during the 5-month observation period. Conventional designations: *—the difference between the IF values of the NBC and Tr groups is significant ($p < 0.05$; Mann–Whitney U-Test).

Test). Significant changes ($p < 0.05$; by the Wilcoxon Matched Pairs Test) in the V_{IF} value, as compared to the first week, were recorded, among others, for the sixth week and for the second to seventh month of observation, as well as in comparing the values of the fifth week with fourth one, those of the sixth week with the third week and the fifth one, and the values of the third to seventh month with those of the fifth week. The V_{IF} values for the fifth week appeared to be another significant extremum and reached 2.2 ± 0.6 points/wk. The

mean V_{IF} values in the Tr group for the first 8 weeks and the entire observation period were equal to 0.3 ± 0.2 and 0.2 ± 0.1 points/wk., respectively.

One week after the injury modelling, the IF in the Fb group ($n = 6$) was 6.7 ± 1.3 points of BBB, not differing significantly from the IF of the Tr group ($p > 0.05$; by the Mann–Whitney U-Test; Fig. 2). Substantial increases in the IF ($p < 0.05$, as compared to the values of the previous observation term; by the Wilcoxon Matched Pairs Test) were recorded during the next week. No significant changes in the IF level were recorded during the entire subsequent period; i.e., starting from the third week to the end of the experiment, the IF values significantly differed only from the IF level at the end of the first week. Actually, the value of the ninth month was characterized by a significant difference from that of the seventh week towards its end ($p < 0.05$; by the Wilcoxon Matched Pairs Test), which was the group maximum for the entire observation period (12.4 ± 1.5 points of BBB). This confirms a significant regress in the IF value towards the end of the experiment, reaching 10.3 ± 2.0 points of BBB within 9 months after the injury modelling. No significant differences were recorded in the IF values in any of the observation terms in the Fb and Tr groups ($p > 0.05$; by the Mann–Whitney U-Test).

The maximum V_{IF} values in the Fb group, which were recorded within the first 2 weeks, were equal, respectively, to 6.7 ± 1.3 and 4.0 ± 1.0 points of BBB. The mean V_{IF} values for the first 8 weeks and the entire observation period reached, respectively, 1.4 ± 0.3 and 0.8 ± 0.2 points/wk., significantly overweighing the mean indicator for the first eig8ht weeks in the Tr group ($p < 0.05$; Mann–Whitney U-Test). Significant differences from the value of the first week were demonstrated by the V_{IF} values during all the subsequent observation terms, while differences from the second week values were recorded at the fourth to sixth weeks and the second to sixth months, and a significant difference was also recorded between the eighth week and the third month ($p < 0.05$; Wilcoxon Matched Pairs Test). No significant differences between the V_{IF} values of the Fb and Tr groups were recorded during any term of observation ($p > 0.05$; Mann–Whitney U-Test).

The IF values in the NBC group ($n = 9$) during the entire observation period proved to be close to those in the Fb group, showing no significant difference ($p > 0.05$; Mann–Whitney U-Test; Fig. 2). After 1 week, the IF in the group became 8.6 ± 1.7 points of BBB, a significant difference from this value was recorded at 3, 4, and 8 weeks as well as at 3, 5, and 6 months after the injury modelling ($p < 0.05$; Wilcoxon Matched Pairs Test). No other differences between the IF values were recorded for different observation terms. The actual maximum of the mean IF value in the NBC group was recorded at 6 weeks after the injury modelling, becoming 10.7 ± 1.6 points of BBB by the end of the ninth month of observation.

Despite the evidently close IF values in the NBC and Fb groups during the entire experiment and the absence of significant differences between the IF values in the Fb and Tr groups, significant differences between the IF values of the NBC and Tr groups were recorded at 2 and 4 weeks as well as 2, 3, and 5 months after injury ($p < 0.05$; Mann–Whitney U-Test; Fig. 2). Considering the methodological shortcomings of the investigation (as mentioned above), the result of the comparative analysis at 4 weeks and 3 months after injury was conventionally significant.

The maximum V_{IF} values in the NBC group were recorded within the first 2 weeks of observation (8.6 ± 1.7 and 1.9 ± 1.1 points/wk., respectively), and the significant difference from the V_{IF} value within the first week was identified for all subsequent observation terms ($p < 0.05$; by the Wilcoxon Matched Pairs Test). The negative V_{IF} value (−1.3 ± 0.9 points/wk.) recorded for the seventh week significantly differed from that of the third week (0.7 ± 0.5 points/wk.; $p < 0.05$, by the Wilcoxon Matched Pairs Test). Significant differences between the V_{IF} values in the NBC and Fb groups were recorded only for the eighth week of observation (in favor of the NBC group; $p < 0.05$; by the Mann–Whitney U-Test) and when comparing the NBC and Tr groups during the fifth week of observation (in favor of the Tr group, by the Mann–Whitney U-Test). The mean V_{IF} values for both the first 8 weeks and the entire observation period in the NBC group were equal, respectively, to 1.4 ± 0.2 and 0.9 ± 0.1 points/wk., significantly overweighing the mean indicator for the first 8 weeks in the Tr group ($p < 0.05$; by the Mann–Whitney U-Test).

The interesting IS dynamics specificity in all three groups was the almost complete absence of significant changes during the entire experiment (Fig. 3). For example, the paretic hindlimb IS value in the Tr group reached 0.7 ± 0.1 points on the Ashworth scale within 1 week after the injury modelling; during the next week, a double, albeit insignificant, increase in the indicator was observed up to the maximum 1.4 ± 0.3 points on the Ashworth scale among all groups and observation terms, which also proved to be characteristic of the end of the fourth experimental week (Fig. 3). Significant differences were recorded only in comparing the values for the eighth week (0.7 ± 0.2 on the Ashworth scale) and those for the third week (1.2 ± 0.2 points on the Ashworth scale; $p = 0.03$, by the Wilcoxon Matched Pairs Test). The IS values for two remaining observation terms (from the end of the fifth to the beginning of the eighth month of observation) were identical and equal to 1.2 ± 0.3 points on the Ashworth scale. During the entire experiment, the IS values in the Tr group insignificantly ranged from 0.7 ± 0.1 to 1.4 ± 0.0 points on the Ashworth scale (Fig. 3).

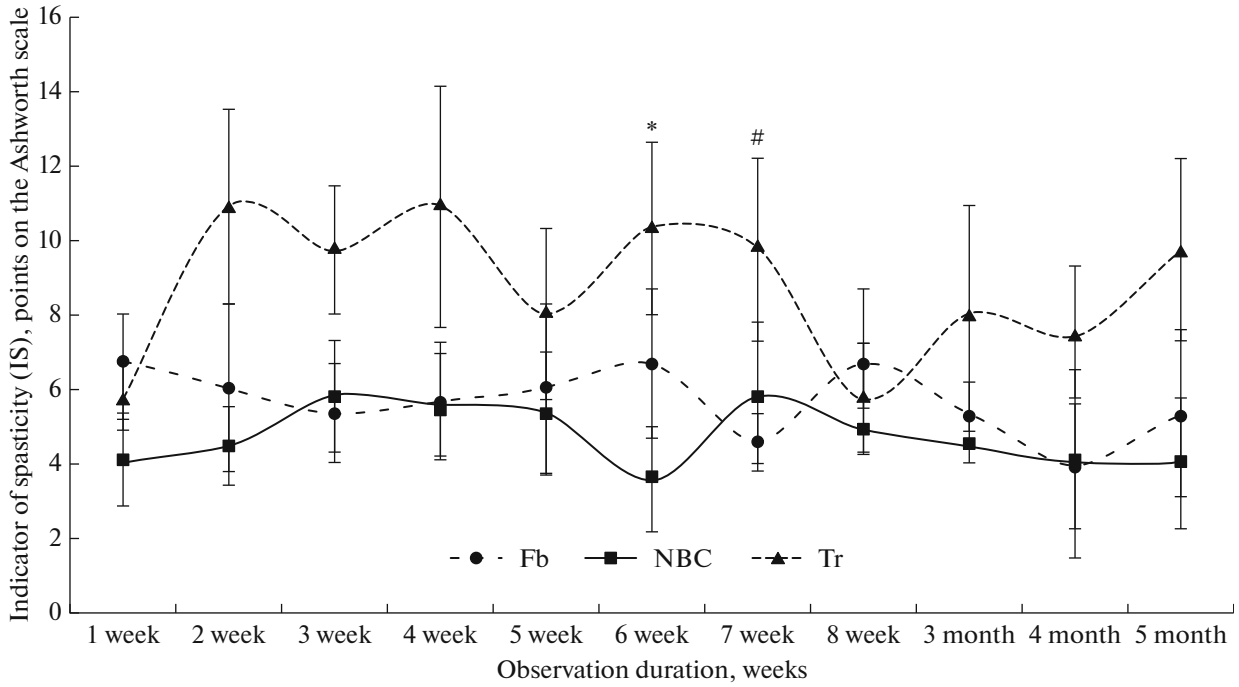

Fig. 3. Dynamics of the indicator of spasticity (IS) in the paretic hindlimb of animals from experimental groups during the 5-month observation period. Conventional designations: *—the difference between the IS values of the NBC and Tr groups is significant ($p < 0.05$; Mann–Whitney U-Test); #—the difference between the IS values of the Fb and Tr groups is significant ($p < 0.05$; Mann–Whitney U-Test).

The V_{IS} values within the first 2 weeks in the Tr group proved to be the highest (0.7 ± 0.1 points/wk. and 0.6 ± 0.3 points/wk., respectively) and varied further about the null point with different amplitudes. A significant difference was determined when comparing the V_{IS} values for the first week of observation and those for the fifth and seventh week, for the second to seventh month ($p < 0.05$; by the Wilcoxon Matched Pairs Test), as well as when the V_{IS} values in the second and the eighth week were compared ($p < 0.05$; Wilcoxon Matched Pairs Test). The mean V_{IS} values for the first 8 months and the entire observation period in the Tr group reached 0.1 ± 0.0 points/wk.

In the Fb group, no substantial IS changes were recorded during the entire observation period ($p > 0.05$; by the Wilcoxon Matched Pairs Test), and the indicator values varied from 0.5 ± 0.02 to 0.8 ± 0.2 points on the Ashworth scale (Fig. 3). A significant difference from the first week's IS value was recorded in the Tr group only at 7 weeks after injury ($p < 0.05$; by the Mann–Whitney U-Test; Fig. 3). The highest V_{IS} value was recorded for the first week of observation (0.8 ± 0.2 points/wk.), but the indicator value further varied near the zero level. A significant difference was recorded when the V_{IS} value for the first week was compared with those for the third and seventh week or for the third and ninth month ($p < 0.05$; by the Wilcoxon Matched Pairs Test), when comparing the V_{IS} values for the second and fourth month, and when comparing the values for the ninth month with those for the seventh week and the third, fourth, and sixth months of observation ($p < 0.05$; the Wilcoxon Matched Pairs Test). No significant differences between V_{IS} values of the Fb and Tr groups were recorded during 5 months of observation. The mean V_{IS} value for the first 8-week period and the entire observation in the Fb group was equal to 0.1 ± 0.0 points/wk., not differing from the mean value of the indicator for the first 8-week period in the Tr group ($p > 0.05$; by the Mann–Whitney U-Test).

During the experiment, the IS values in the NBC group varied from 0.4 ± 0.2 to 0.7 ± 0.2 points on the Ashworth scale (Fig 3), despite the fact that a significant difference was recorded only between the values for the third and sixth week of observation ($p < 0.05$; by the Wilcoxon Matched Pairs Test). No significant differences were recorded during the experiment between the IS values of the NBC and Fb groups ($p > 0.05$; by the Mann–Whitney U-Test), but significant differences between the NBC and Tr groups were recorded only during the sixth week of observation ($p < 0.05$; by the Mann–Whitney U-Test). The maximum V_{IS} value (0.5 ± 0.1 points/wk.) was recorded in the NBC group after the first experimental week. The values of this indicator in the NBC group for all the subsequent observation terms (except the values during the third and seventh week) were significantly lower ($p < 0.05$; by the Wilcoxon Matched Pairs Test). Apart from this, the V_{IS} values during the sixth week

were significantly lower than those for the third week, the V_{IS} values during the seventh week were significantly higher than those of the fourth or fifth week and the fourth month, whereas the eighth month values were significantly higher than those of the third and fifth months ($p < 0.05$ for all the mentioned cases; by the Wilcoxon Matched Pairs Test). A significant difference in the NBC group's V_{IS} value was recorded only for the seventh week in its comparison with the Fb group values (in favor of the NBC group; $p < 0.05$; by the Wilcoxon Matched Pairs Test). The mean V_{IS} value for the first 8 weeks and the entire observation period reached, respectively, 0.1 ± 0.0 and 0.0 ± 0.0 points/wk., not differing ($p > 0.05$; by the Mann–Whitney U-Test) from the mean indicator for the first 8-week period in the Tr group (compared only with the corresponding indicator of the NBC group) and the Fb group (compared with both corresponding indicators of the NBC group).

During the analysis of the mean IF and IS values, V_{IF} and V_{IS}, a significant negative correlation with the indicator for the observation duration was identified for V_{IF} of the Fb group ($r = -0.72$) and the NBC group ($r = -0.63$) ($p < 0.05$; Spearman Rank Order Correlations Test). During the analysis of individual IF and IS values, an essential negative correlation was found in the Tr group at 1 and 2 weeks and 4, 5, and 7 months after injury ($r = \leq -0.80$; $p < 0.05$; Spearman Rank Order Correlations Test); at 4, 5, and 6 weeks and 2 and 5 months after injury in the Fb group ($r \leq -0.85$; $p < 0.05$; Spearman Rank Order Correlations Test); and at 1, 3 to 8 weeks and 4–9 months after injury in the NBC group ($r \leq -0.68$; $p < 0.05$; Spearman Rank Order Correlations Test). During the analysis of individual V_{IF} and V_{IS} values, a substantial negative correlation was recorded in the Tr group at 1, 6, and 7 weeks and at 3 months after injury ($r \leq -0.77$; $p < 0.05$; Spearman Rank Order Correlations Test), at 6 weeks and 5 months after injury in the Fb group ($r \leq -0.88$; $p < 0.05$; Spearman Rank Order Correlations Test), and only at 1 week after injury in the NBC group ($r = -0.72$; $p < 0.05$; Spearman Rank Order Correlations Test). Actually, no significant negative correlation was recorded for the mean IF and IS or V_{IF} and V_{IS} values during the experiment in each of the groups ($r > -0.48$; $p < 0.05$; Spearman Rank Order Correlations Test).

The obtained results confirm that the implantation of a fibrin matrix with incorporated neonatal brain cells and without the latter into the SCI epicenter has a substantial effect on the SCI treatment course, promoting the recovery of the locomotor function in a paretic hindlimb. Further experimental research with significantly larger samples is required to evaluate the importance of the positive role shared by the cells involved in this study.

Pathohistological picture of the injury area in the animals of experimental groups in the remote injury period. According to the investigations of silver-impregnated specimens (Fig. 4), the histological picture in the injury focus and its perifocal area in the remote posttraumatic observation period showed the substitution of the deficiency area by elements of glia and connective tissue, which formed a gliofibrous scar conglomerate (Tr, Fb, and NBC groups, Figs. 4a, 4b). Individual, seemingly, newly-formed, nerve fibers (Tr, Fb, and NBC groups, Fig. 4c) were visualized in the superficial scar regions near the meninges (Tr and Fb groups) as well as in near the scar area of the spinal cord. The pathomorphological data show that one of the possible mechanisms underlying the recovery of the motor function in the posttraumatic paretic hindlimb, including due to the implantation of a fibrin matrix, is the overgrowth of nerve fibers through the organization region of the injured spinal cord substance. The important role of this mechanism in creating a positive effect of the fibrin matrix implantation may possibly be clarified through an extended morphometric analysis.

DISCUSSION

SCI, despite its low morbidity, is a widespread cumulative pathology, which substantially degrades the quality of life in those injured and is associated with a significant economic burden (DeVivo, 2912; Oliveri et al., 2014; Pretz et al., 2016; GBD 2016 Traumatic Brain Injury and Spinal Cord Injury Collaborators, 2019). The key impairment of SCI-caused neurological deficiency is a lesion of the long nerve fibers transmitting impulses from the brain to the efferent neurons of the spinal cord. The pathogenesis of a typical SCI includes a set of predominantly sequential processes (Tran et al., 2018; Alizadeh et al., 2019), which are regulated by a wide spectrum of intercellular interaction factors, in particular, by cytokines (Garcia et al., 2016) and growth factors (Ko et al., 2019). Despite the actively studied limitations in the regeneration of SCI-impaired axons (Rao and Pearse, 2016; Tran et al., 2018; Swieck et al., 2019), there are descriptions of a mild autogenous brain motor system regeneration (Steeves, 2015; Khorasanizadeh et al., 2019), which is most probably provided by rearranging the topology of neural networks, such as, propriospinal neurons (Blesch and Tuszynski, 2009; Flynn et al., 2011; Brown and Martinez, 2019). In this sense, the strategy aimed to develop methods for reconstructing neural networks proceeds from certain premises (Liu et al., 2018; Wang et al., 2018; Liu et al., 2019; Zhang et al., 2019; Cizkova et al., 2020; Shah et al., 2020).

Our data on the effectiveness of transplanting NBCs associated with a fibrin matrix into the rat SCI area wholly agree with the results obtained by another group (Lu et al., 2012), in fact, in modelling a full incision of an adult rat's spinal cord at the upper thoracic level (T_3). Similarly, the allotransplantation of rat fetal spinal cord neural stem cells (E14) into the injury area 2 weeks after its modelling in complex with a fibrin matrix artificially saturated with numerous growth

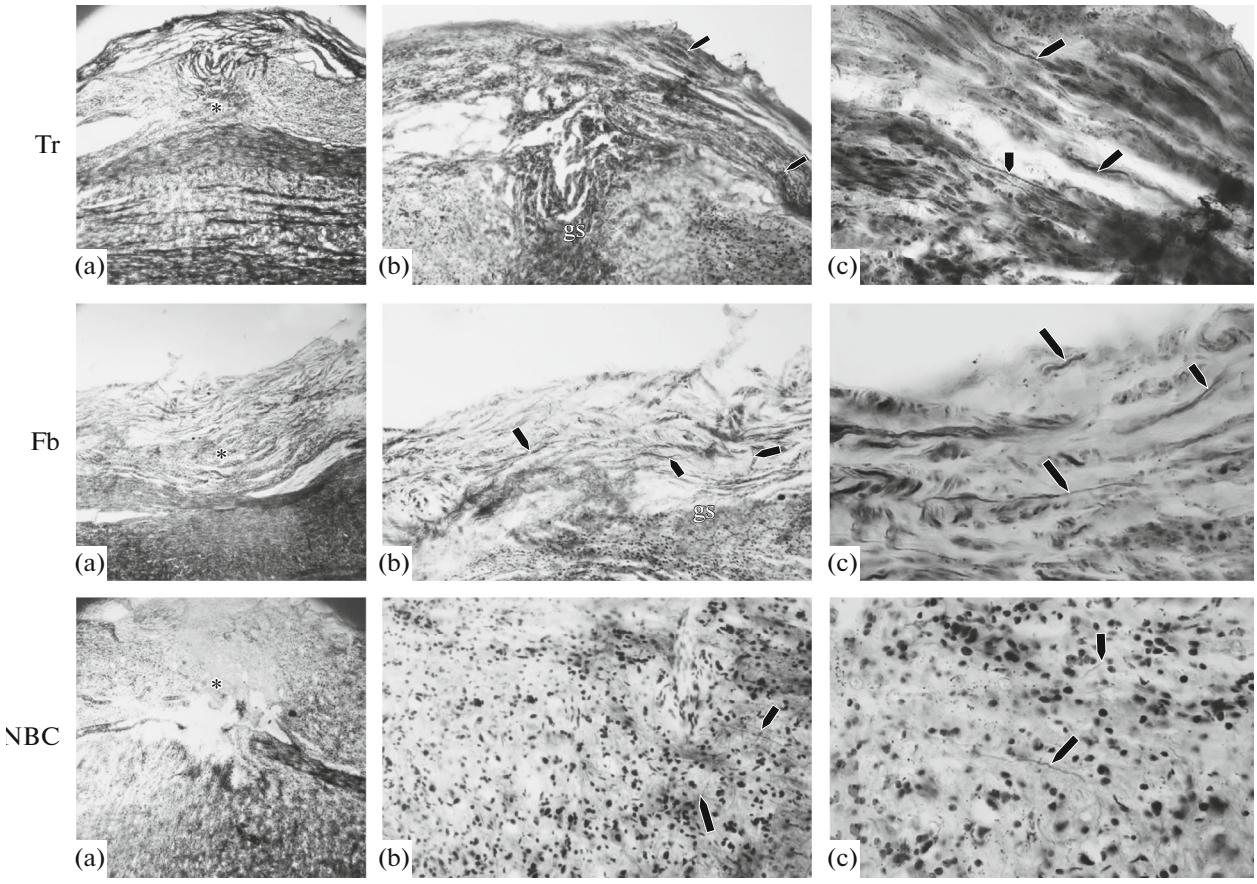

Fig. 4. Histological picture of the injury focus and the perifocal area in the remote injury period by the investigations of spinal cord longitudinal sections impregnated with silver nitrate. Newly formed small nerve fibers (indicated by arrows) amid the thickened connective-tissue cover of the spinal cord near the organized injury area (Tr), as well as in the thickness of the scar tissue, which, most probably, replaced the fibrin implant (Fb), and in the spinal cord substance, near the fibrin matrix implantation region (NBC). Conventional designations: *—the injury epicenter (Tr, Fb, and NBC) and the fibrin matrix implantation (Fb and NBC); →—nerve fibers; gs—gliofibrous scar. Scale: (a) 200 μm, (b) 20 μm, and (c) 10 μm.

factors and the calpain inhibitor contributes to a 5-point improvement in the hindlimb function, as compared to the reference group (isolated injury), i.e., approximately, from 2 to 7 points of BBB. We recorded an analogous significant 5-point difference between the IF values in the NBC (10.7 ± 1.6 points of BBB) and Tr groups (6.0 ± 1.7 points of BBB), which, however, most probably resulted from the very presence of the fibrin matrix in the injury area, and the significant efficiency of the matrix-associated NBCs transplantation, as compared to the implantation of the NBCs-free matrix, had, evidently, only statistical substantiation.

At the same time, another study (Johnson et al., 2010) did not record any significant positive effect of a fibrin complex implanted into the region of the dorsal spinal cord hemisection performed in an adult rat at the T_9 level within 2 or 4 weeks after the injury modelling. The authors did not, in fact, support their conclusion by quantitative illustrations, which complicated its interpretation, since the recovery of the hindlimb motor function in rat after this kind of spinal cord injury without any repair interventions reached 11 points of BBB already within 1 month (Majczynski and Slavinska, 2007).

Nevertheless, it is suggested that our data should, first of all, be discussed through the prism of possible mechanisms underlying the effect of a fibrin matrix on the SCI recovery course. The obtained results have confirmed that the fibrin matrix implantation has a positive effect within the very initial SCI period, since the IF advantage in the Fb and NBC groups over this indicator in the Tr group was recorded already from the first observation term (less expressed in the Fb group within this term) and its value was maintained at the same high level throughout the entire observation period. One of the probable mechanisms underlying this effect consists, in our opinion, in the antihemorrhagic effect of fibrin during the spinal cord injury, due to which, a direct contact of the brain substance with blood and liquor, and, therefore, with the immune system, its regional control elements, and its

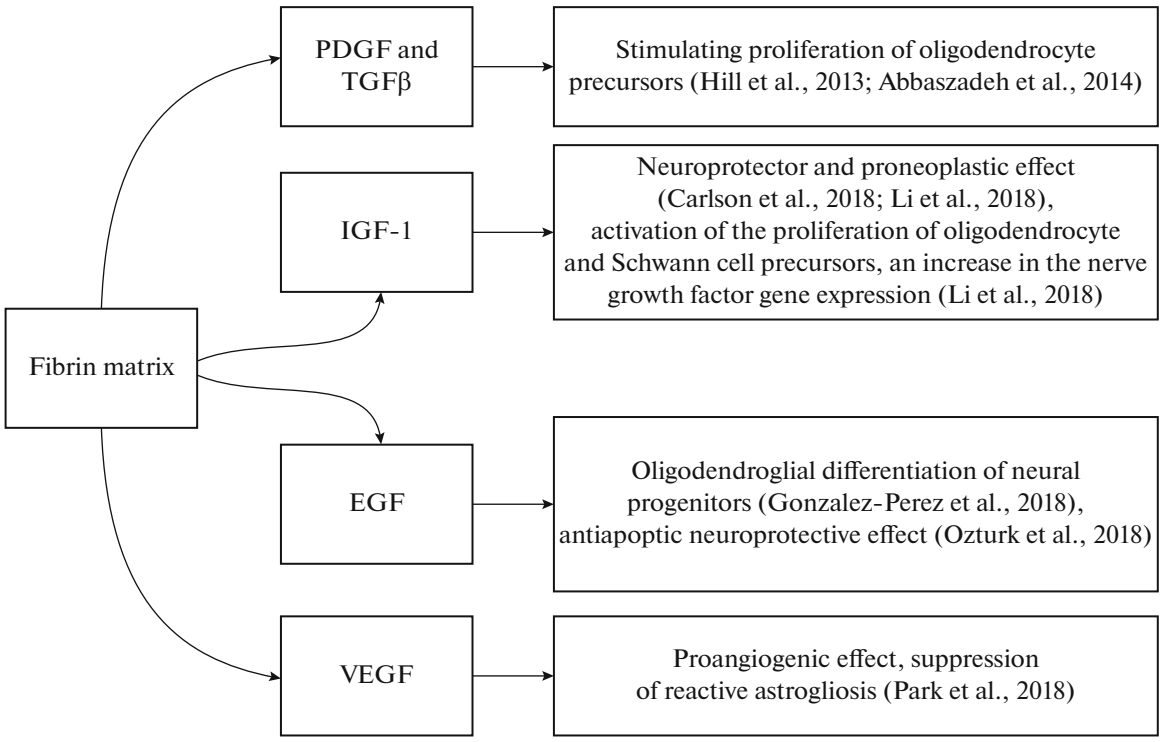

Fig. 5. Effects produced by the main neurotrophic factors of fibrin matrices according to the literature.

triggers of the secondary inflammatory lesion was limited. Another possible mechanism may be related to the action of the matrix-associated regulatory factors, including those produced by the presence of NBCs. It is known that the association of polymerized fibrin derived due to plasma coagulation contains thrombocytes (Tatullo et al., 2012), a source of the growth factors, such as platelet-derived growth factor (PDGF), transforming growth factor β (TGFβ), insulin-like growth factor (IGF), vascular endothelial growth factor (VEGF), and epidermal growth factor (EGF) (Amable et al., 2013; Hotwani et al., 2014; Yao et al., 2016), which, in any case, may affect the course of local tissue responses in the most acute SCI period. Remote effects of the propriospinal growth factors are also probable—for example, some studies described the oligodendrocyte precursor proliferation stimulation for PDGF and TGFβ (Hill et al., 2013; Abbaszadeh et al., 2014); the neuroprotector and proneuroplastic effect (Carlson et al., 2018; Li et al., 2018), the proliferation activation of oligodendrocyte and Schwann cell precursors, and an increase in the expression of nerve growth factor gene (Li et al., 2018) for IGF-1; oligodendroglial differentiation of neural progenitors (Gonzalez-Perez et al., 2009) and antiapoptotic neuroprotector effect (Ozturk et al., 2018) for EGF; and the suppression of reactive astrogliosis, apart from the well-known proangiogenic effect, was described for VEGF (Park et al., 2018). In addition, the nerve fibers incorporated into the fibrin matrix are known to preserve their neural markers, especially, β-III tubulin, NF-200 (Bento et al., 2017) and, first of all, to be able to participate in the regenerative process. The reality of these suggestions needs to be confirmed by further detailed research.

One of the essential problems for regenerative medicine is the unsatisfactory clinical translation of experimental data (Blesch and Tuszynski, 2009; Lemmon et al., 2014). This is, first of all, related to low effectiveness of the studied regenerative interventions and the absence of certified experimental protocols for this kind of studies (Lemmon et al., 2014; Assinck et al., 2017; Dietz and Schwab, 2017). The typical form of SCI for clinical conditions, euthanasia, (Assinck et al., 2017; Dietz and Schwab, 2017; Alizadeh et al., 2019) does not allow experimenters to assess the rehabilitation efficacy of substantial transplants, while modelling a full spinal cord incision has to deal with the postsurgery difficulties in the management of experimental animals. This caused us to choose a unilateral rat spinal cord hemisection as an SCI model. In addition, the choice of the matrix implantation time was substantiated in this study by the fact that the maximum activity of autogenic neuroplastic process is within the first weeks after the SCI (Blesch and Tuszynski, 2009) as well as by the local inflammatory response and secondary alteration dynamics (Tran et al., 2018; Alizadeh et al., 2019), which were always accompanied by an increase in the cytokine concen-

tration and other chemical factors affecting the state of transplanted cells.

Technical precautions of the study. The BBB scale used by us to assess the locomotor function of the paretic hindlimb was developed for studying consequences of a bilateral spinal cord injury (Basso et al., 1995). Despite the long practice of its use for unilateral injuries (Metz et al., 2000; Mills et al., 2001; Webb and Muir, 2002; Arvanian et al., 2009; Hsieh et al., 2010; Pertici et al., 2013; Zhao et al., 2015; Zhang et al., 2016; Li et al., 2017), in our opinion, the verification potential of the scale for these conditions is limited. Apart from the expediency to attract kinematic and audiologic analysis of the recorded video material, determining a correct IF value is complicated by compensating for the motor deficiency manifestations in the paretic hindlimb, which are used as differential criteria on the BBB scale at above the 7-point level. In particular, this is related to the plantar placement during the stance phase, the weight support of the corresponding trunk quadrant by the hindlimb, the forelimb-hindlimb coordination, the adequate toe clearance, and the paw position during surface locomotion at different stance phase stages during the stepping cycle as well as to the translateral trunk locomotor instability and the maintenance of the tail during surface locomotion. The negative consequences of these methodological shortcomings, in our opinion, are partly compensated for by the observance of the same methodological and technological conditions in the IF assessment in all compared experimental groups.

The methodological problems in the Ashworth scale include complexity in the verification of the mild spastic paresis (we used the original criteria) and subjective differentiation between the IS assessments in the interval from 1 to 3 points in small experimental animals. In particular, the effectiveness of reducing the muscle tone associated with the tested animal's ordinary behavioral activity by using tricks, such as "blinding" the animal with the experimenter's hand, and preliminary acclimatization (Dong et al., 2005), in our opinion, is doubtful. Our choice of the Ashworth scale for spasticity assessment was caused by the limited informativeness of the alternative technically complicated electroneuromyography (ENMG) instrument. More so, we know that additional correlation between the spasticity levels assessed on the Ashworth scale and ENMG assessments is significantly weak (Dong et al., 2005), whereas the main ENMG indicators show rather significant interpersonal and time variability (Cliffer et al., 1998), which is most probably caused by difficulties in identifying the so-called muscle motor point in small experimental animals, especially, in view of the decomposition and changes in the fiber structure of the paretic muscles after SCI (D'Amico et al., 2014).

In general, excluding the mentioned precautions and taking into account the IF difference value in the NBC and Tr groups, the data obtained in this study can be considered sufficiently significant.

CONCLUSIONS

The fibrin matrix promotes the viability, growth, and differentiation of the incorporated neonatal rat brain cells. With implantation of either an empty fibrin matrix or a matrix filled with neonatal rat brain cells, the level of the motor function reaches approximately 11 points of BBB, overvaluing the reference group almost by 5 points of BBB, and, especially significantly, due to the presence of allogeneic neonatal brain cells. Implantation of either an empty fibrin matrix or a matrix filled with neonatal brain cells significantly reduces the spasticity of the paretic hindlimb in the intermediary period of injury. Thus, the immediate implantation of a fibrin matrix in complex with neonatal brain cells or without the latter has a significant positive effect on the recovery of the motor function after a spinal cord injury.

FUNDING

This study was not supported by any grant from financial establishments of the governmental, commercial, or noncommercial sectors.

COMPLIANCE WITH ETHICAL STANDARDS

Conflict of interests. The authors declare that they have no conflict of interests.

Statement on the welfare of animals. The study observed all standards of bioethics and humane treatment of animals, which were stipulated under the EU Council Directive 86/609/EEC On the Approximation of Laws, Regulations, and Administrative Provisions of the Member States regarding the Protection of Animals Used for Experimental and Other Scientific Purposes (1986), the European Convention for the Protection of Vertebrate Animals Used for Experimental and Other Scientific Purposes (1986), and Ukrainian Law no. 3447-IV On the Protection of Animals from Cruelty (2006). The investigations were sanctioned by the Commission on Bioethics of the Romodanov Neurosurgery Institute, National Academy of Medical Sciences of Ukraine (protocol no. 30 of April 11, 2019).

REFERENCES

Abbaszadeh, H.-A., Tiraihi, T., Delshad, A., et al., Differentiation of neurosphere-derived rat neural stem cells into oligodendrocyte-like cells by repressing PDGF-α and Olig2 with triiodothyronine, *Tissue Cell*, 2014, vol. 46, no. 6, pp. 462–469. https://doi.org/10.1016/j.tice.2014.08.003

Amable, P.R., Carias, R.B.V., Teixeira, M.V.T., et al., Platelet-rich plasma preparation for regenerative medicine: optimization and quantification of cytokines and growth factors, *Stem Cell Res. Ther.*, 2013, vol. 4, no. 3,

art. ID 67.
https://doi.org/10.1186/scrt218

Arvanian, V.L., Schnell, L., Lou, L., et al., Chronic spinal hemisection in rats induces a progressive decline in transmission in uninjured fibers to motoneurons, *Exp. Neurol.*, 2009, vol. 216, no. 2, pp. 471–480.
https://doi.org/10.1016/j.expneurol.2009.01.004

Assinck, P., Duncan, G.J., Hilton, B.J., et al., Cell transplantation therapy for spinal cord injury, *Nat. Neurosci.*, 2017, vol. 20, no. 5, pp. 637–647.
https://doi.org/10.1016/j.stemcr.2020.05.017

Basso, D.M., Beattie, M.S., and Bresnahan, J.C., A sensitive and reliable locomotor rating scale for open field testing in rats, *J. Neurotrauma*, 1995, vol. 12, no. 1, pp. 1–21.
https://doi.org/10.1089/neu.1995.12.1

Bento, A.R., Quelhas, P., Oliveira, M.J., et al., Three-dimensional culture of single embryonic stem-derived neural/stem progenitor cells in fibrin hydrogels: neuronal network formation and matrix remodeling, *J. Tissue Eng. Regen. Med.*, 2017, vol. 11, no. 12, pp. 3494–3507.
https://doi.org/10.1002/term.2262

Blesch, A. and Tuszynski, M.H., Spinal cord injury: plasticity, regeneration and the challenge of translational drug development, *Trends Neurosci.*, 2009, vol. 32, no. 1, pp. 41–47.
https://doi.org/10.1016/j.tins.2008.09.008

Brown, A. and Martinez, M., From cortex to cord: motor circuit plasticity after spinal cord injury, *Neural Regener. Res.*, 2019, vol. 14, no. 12, pp. 2054–2062.
https://doi.org/10.4103/1673- 5374.262572

Burns, A.S., Marino, R.J., Kalsi-Ryan, S., Middleton, J.W., Tetreault, L.A., Dettori, J.R., Mihalovich, K.E., and Fehlings, M.G., Type and timing of rehabilitation following acute and subacute spinal cord injury: a systematic review, *Global Spine J.*, 2017, vol. 7, no. 3, 175–194.
https://doi.org/10.1177/2192568217703084

Cargnello, M. and Roux, P.P., Activation and function of the MAPKs and their substrates, the MAPK-activated protein kinases, *Mol. Biol. Rev.*, 2011, vol. 75, no. 1, pp. 50–83.
https://doi.org/10.1128/MMBR.00031-10

Carlson, S.W. and Saatman, K.E., Central infusion of IGF-1 increases hyppocampal neurogenesis and improves neurobehavioral function following traumatic brain injury, *J. Neurotrauma*, 2018, vol. 35, no. 13, pp. 1467–1480.
https://doi.org/10.1089/neu.2017.5374

Carriel, V., Garrido-Gomez, J., Hernandez-Cortes, P., et al., Combination of fibrin-agarose hydrogels and adipose-derived mesenchymal stem cells for peripheral nerve regeneration, *J. Neural Eng.*, 2013, vol. 10, no. 2, art. ID 026022.
https://doi.org/10.1088/1741-2560/10/2/026022

Carriel, V., Scionti, G., Campos, F., et al., *In vitro* characterization of a nanostructered fibrin agarose bio-artificial nerve substitute, *J. Tissue Eng. Regener. Med.*, 2015, vol. 11, no. 5, pp. 1412–1426.
https://doi.org/10.1002/term.2039

Cizkova, D., Murgoci, A.N., and Cubinkova, V., Spinal cord injury: animal models, imaging tools and the treatment strategies, *Neurochem. Res.*, 2020, vol. 45, no. 1, pp. 134–143.
https://doi.org/10.1007/s11064-019-02800-w

Cliffer, K.D., Tonra, J.R., Carson, S.R., et al., Consistent repeated M- and H-wave recording in the hind limb of rats, *Muscle Nerve*, 1998, vol. 21, no. 11, pp. 1405–1413.
https://doi.org/10.1002/(sici)1097-4598(199811)21:11<1405::aidmus7>3.0.co;2-d

D'Amico, J.M., Condliffe, E.G., Martins, K.J., et al., Recovery of neuronal and network excitability after spinal cord injury and implications for spasticity, *Front. Integr. Neurosci.*, 2014, vol. 8, art. ID 36.
https://doi.org/10.3389/fnint.2014.00036

DeVivo, M.J., Epidemiology of traumatic spinal cord injury: trends and future implications, *Spinal Cord*, 2012, vol. 50, no. 5, pp. 365–372.
https://doi.org/10.1038/sc.2011.178

Dietz, V. and Schwab, M.E., From the rodent spinal cord injury model to human application: promises and challenges, *J. Neurotrauma.*, 2017, vol. 34, no. 9, pp. 1826–1830.
https://doi.org/10.1089/neu.2016.4513

Dijkers, M.P., Akers, K.G., and Dieffenbach, S., Systematic reviews of clinical benefits of exoskeleton use for gait and mobility in neurologic disorders: a tertiary study, *Arch. Phys. Med. Rehabil.*, 2021, vol. 102, no. 2, pp. 300–313.
https://doi.org/10.1016/j.apmr.2019.01.025

Dong, H.W., Wang, L.H., Zhang, M., et al., Decreased dynorphin A (1–17) in the spinal cord of spastic rats after the compressive injury, *Brain Res. Bull.*, 2005, vol. 67, no. 3, pp. 189–195.
https://doi.org/10.1016/j.brainresbull.2005.06.026

Finnerup, N.B., Norrbrink, C., Trok, K., et al., Phenotypes and predictors of pain following traumatic spinal cord injury: a prospective study, *J. Pain*, 2014, vol. 15, no. 1, pp. 40–48.
https://doi.org/10.1016/j.jpain.2013.09.008

Flynn, J.R., Graham, B.A., Galea, M.P., et al., The role of propriospinal interneurons in recovery from spinal cord injury, *Neuropharmacology*, 2011, vol. 60, no. 5, pp. 809–822.
https://doi.org/10.1016/j.neuropharm.2011.01.016

Garcia, E., Aguilar-Cevallos, J., Silva-Garcia, R., et al., Cytokine and growth factor activation in vivo and in vitro after spinal cord injury, *Mediators Inflammation*, 2016, vol. 2016, art. ID 9476020.
https://doi.org/10.1155/2016/9476020

GBD 2016 Traumatic Brain Injury and Spinal Cord Injury Collaborators, Global, regional, and national burden of traumatic brain injury and spinal cord injury, 1990–2016: a systematic analysis for the Global Burden of Disease Study, *Lancet Neurol.*, 2019, vol. 18, no. 1, pp. 56–87.
https://doi.org/10.1016/S1474-4422(18)30415-0

Gilerovich, E.G., Moshonkina, T.R., Fedorova, E.A., et al., Morphofunctional characteristics of the lumbar enlargement of the spinal cord in rats, *Neurosci. Behav. Physiol.*, 2008, vol. 38, no. 8, pp. 855–860.
https://doi.org/10.1007/s11055-008-9056-8

Gonzalez-Perez, O., Romero-Rodriguez, R., Soriano-Navarro, M., et al., Epidermal growth factor induces the progeny of subventricular zone type B cells to migrate and differentiate into oligodendrocytes, *Stem Cells*, 2009, vol. 27, no. 8, pp. 2032–2043.
https://doi.org/10.1002/stem.119

Hamid, R., Averbeck, M.A., Chiang, H., et al., Epidemiology and pathophysiology of neurogenic bladder after spinal cord injury, *World J. Urol.*, 2018, vol. 36, no. 10,

pp. 1517–1527.
https://doi.org/10.1007/s00345-018-2301-z

Hill, R.A., Patel, K.D., Medved, J., et al., NG2 cells in white matter but not gray matter proliferate in response to PDGF, *J. Neurosci.*, 2013, vol. 33, no. 36, pp. 14558–14566.
https://doi.org/10.1523/JNEUROSCI.2001-12.2013

Holtz, K.A., Lipson, R., Noonan, V.K., et al., Prevalence and effect of problematic spasticity after traumatic spinal cord injury, *Arch. Phys. Med. Rehabil.*, 2017, vol. 98, no. 6, pp. 1132–1138.
https://doi.org/10.1016/j.apmr.2016.09.124

Hotwani, K. and Sharma, K., Platelet rich fibrin—a novel acumen into regenerative endodontic therapy, *Restor. Dent. Endod.*, 2014, vol. 39, no.1, pp. 1–6.
https://doi.org/10.5395/rde.2014.39.1.1

Hsieh, T.H., Tsai, J.Y., Wu, Y.N., et al., Time course quantification of spastic hypertonia following spinal hemisection in rats, *Neuroscience*, 2010, vol. 167, no. 1, pp. 185–198.
https://doi.org/10.1016/j.neuroscience.2010.01.064

Jeong, H.J., Yun, Y., Lee, S.J., et al., Biomaterials and strategies for repairing spinal cord lesions, *Neurochem. Int.*, 2021, vol. 144, art. ID, 104973.
https://doi.org/10.1016/j.neuint.2021.104973

Johnson, P.J., Parker, S.R., and Sakiyama-Elbert, S.E., Fibrin-based tissue engineering scaffolds enhance neural fiber sprouting and delay the accumulation of reactive astrocytes at the lesion in a subacute model of spinal cord injury, *J. Biomed. Mater. Res., Part A*, 2010, vol. 92, no. 1, pp. 152–163.
https://doi.org/10.1002/jbm.a.32343

Khan, S., Mafi, P., Mafi, R., et al., A systematic review of mesenchymal stem cells in spinal cord injury, intervertebral disc repair and spinal fusion, *Curr. Stem Cell Res. Ther.*, 2018, vol. 13, no. 4, pp. 316–323.
https://doi.org/10.2174/1574888x11666170907120030

Khorasanizadeh, M., Yousefifard, M., Eskian, M., et al., Neurological recovery following traumatic spinal cord injury: a systematic review and meta-analysis, *J. Neurosurg. Spine*, 2019, vol. 15, pp. 1–17.
https://doi.org/10.3171/2018.10.SPINE 18802

Ko, C.C., Tu, T.H., Wu, J.C., et al., Acidic fibroblast growth factor in spinal cord injury, *Neurospine*, 2019, vol. 16, no. 4, pp. 728–738.
https://doi.org/10.14245/ns.1836216.108

Kolomiytsev, A.K., Chaikovskiy, I.B., and Tereshchenko, T.L., Rapid method of silver nitrate impregnation of elements of the peripheral nervous system suitable for paraffin and celloidin sections, *Arkh. Anat., Gistol. Embriol.*, 1981, vol. 81, no. 8, pp. 93–96.

Kopach, O., Medvediev, V., Krotov, V., et al., Opposite, bidirectional shifts in excitation and inhibition in specific types of dorsal horn interneurons are associated with spasticity and pain post-SCI, *Sci. Rep.*, 2017, vol. 7, no. 1, art. ID 5884.
https://doi.org/10.1038/s41598-017-06049-7

Lemmon, V.P., Ferguson, A.R., Popovich, P.G., et al., MIASCI Consortium, Minimum information about a spinal cord injury experiment: a proposed reporting standard for spinal cord injury experiments, *J. Neurotrauma*, 2014, vol. 31, no. 15, vol. 1354–1361.
https://doi.org/10.1089/neu.2014.3400

Li, J.A., Zhao, C.F., Li, S.J. et al., Modified insulinlike growth factor 1 containing collagen-binding domain for nerve regeneration, *Neural Regener. Res.*, 2018, vol. 13, no. 2, pp. 298–303.
https://doi.org/10.4103/1673-5374.226400

Li, L.S., Yu, H., Raynald, R., et al., Anatomical mechanism of spontaneous recovery in regions caudal to thoracic spinal cord injury lesions in rats, *PeerJ.*, 2017, vol. 5, art. ID e2865.
https://doi.org/10.7717/peerj.2865

Lin, L., Lin, H., Bai, S., et al., Bone marrow mesenchymal stem cells (BMSCs) improved functional recovery of spinal cord injury partly by promoting axonal regeneration, *Neurochemistry*, 2018, vol. 115, pp. 80–84.
https://doi.org/10.1016/j.neuint.2018.02.007

Litvinov, R.I., Gorkun, O.V., Owen, S.F., et al., Polymerization of fibrin: specificity, strength, and stability of knob-hole interactions studied at the single-molecule level, *Blood*, 2005, vol. 106, no. 9, pp. 2944–2951.
https://doi.org/10.1182/blood-2005-05-2039

Liu, S., Schackel, T., Weidner, N., and Puttagunta, R., Biomaterial-supported cell transplantation treatments for spinal cord injury: challenges and perspectives, *Front. Cell. Neurosci.*, 2018, vol. 11, art. ID 430.
https://doi.org/10.3389/fncel.2017.00430

Liu, S., Xie, Y.Y., and Wang, B., Role and prospects of regenerative biomaterials in the repair of spinal cord injury, *Neural Regener. Res.*, 2019, vol. 14, no. 8, pp. 1352–1363.
https://doi.org/10.4103/1673-5374.253512

Lu, P., Wang, Y., Graham, L. et al., Long-distance growth and connectivity of neural stem cells after severe spinal cord injury, *Cell*, 2012, vol. 150, no. 6, pp. 1264–1273.
https://doi.org/10.1016/j.cell.2012.08.020

Lu, P., Grahman, L., Wang, Y., et al., Promotion of survival and differentiation of neural stem cells with fibrin and growth factor coctails after severe spinal cord injury, *J. Visualized Exp.*, 2014, vol. 89, art. ID e50641.
https://doi.org/10.3791/50641

Majczynski, H. and Slawinska, U., Locomotor recovery after thoracic spinal cord lesions in cats, rats and humans, *Acta Neurobiol. Exp.*, 2007, vol. 67, no. 3, pp. 235–257.

Metz, G.A., Merkler, D., Dietz, V., et al., Efficient testing of motor function in spinal cord injured rats, *Brain Res.*, 2000, vol. 883, no. 2, pp. 165–177.
https://doi.org/10.1016/s0006-8993 (00)02778-5

Mills, C.D., Hains, B.C., Johnson, K.M., et al., Strain and model differences in behavioral outcomes after spinal cord injury in rat, *J. Neurotrauma*, 2001, vol. 18, no. 8, pp. 743– 756.
https://doi.org/10.1089/089771501316919111

Moonen, G., Satkunendrarajah, K., Wilcox, J.T., et al., A New acute impact-compression lumbar spinal cord injury model in the rodent, *J. Neurotrauma*, 2016, vol. 33, no. 3, pp. 278–289.
https://doi.org/10.1089/neu.2015.3937

Muheremu, A., Peng, J., and Ao, Q., Stem cell based therapies for spinal cord injury, *Tissue Cell*, 2016, vol. 48, no. 4, pp. 328–333.
https://doi.org/10.1016/j.tice.2016.05.008

Muller, Ì.F., Ris, I., and Ferry, J.D., Electron microscopy of fine fibrin clots and fine and coarse fibrin films. Observations of fibers in cross-section and in deformed

states, *J. Mol. Biol.*, 1984, vol. 174, no. 2, pp. 369–384. https://doi.org/10.1016/0022-2836(84)90343-7

Oliveri, R.S., Bello, S., and Biering-Sørensen, F., Mesenchymal stem cells improve locomotor recovery in traumatic spinal cord injury: systematic review with meta-analyses of rat models, *Neurobiol. Dis.*, 2014, vol. 62, pp. 338–353. https://doi.org/10.1016/j.nbd.2013.10.014

Olude, M.A., Mustapha, O.A., Ogunbunmi, T.K., et al., The vertebral column, ribs, and sternum of the African giant rat (*Cricetomys gambianus* Waterhouse), *Sci. World J.*, 2013, vol. 2013, art. ID 973537. https://doi.org/10.1155/2013/973537

Ozturk, A.M., Sozbilen, M.C., Sevgili, E., et al., Epidermal growth factor regulate apoptosis and oxidative stress in a rat model of spinal cord injury, *Injury*, 2018, vol. 49, no. 6, pp. 1038–1045. https://doi.org/10.1016/j.injury.2018.03.021

Özkan, Z.E., Macro-anatomical investigations on the skeletons of mole-rat (*Spalax leucodon* Nordmann) III. Skeleton axiale, *Vet. Arhiv*, 2007, vol. 77, pp. 281–289.

Park, M.N., Lee, J.Y., Jeong, M.S., et al., The roll of Purkinje cell-derived VEGF in cerebellar astrogliosis in Niemann-Pick type C mice, *BMB Rep.*, 2018, vol. 51, no. 2, pp. 79– 84. https://doi.org/10.5483/bmbrep.2018.51.2.168

Pertici, V., Amendola, J., Laurin, J., et al., The use of poly(N-(2-hydroxypropyl)-methacrylamide) hydrogel to repair a T10 spinal cord hemisection in rat: a behavioural, electrophysiological and anatomical examination, *ASN Neuro*, 2013, vol. 5, no. 2, art. ID e00114. https://doi.org/10.1042/AN20120082

Pretz, C.R., Kozlowski, A.J., Chen, Y., et al., Trajectories of life satisfaction after spinal cord injury, *Arch. Phys. Med. Rehabil.*, 2016, vol. 97, no. 10, pp. 1706–1713. https://doi.org/10.1016/j.apmr.2016.04.022

Robinson, J. and Lu, P., Optimization of trophic support for stem cell graft in sites of spinal cord injury, *Exp. Neurol.*, 2017, vol. 291, pp. 87–97. https://doi.org/10.1016/j.exp neurol.2017.02.007

Rao, S.N. and Pearse, D.D., Regulating axonal responses to injury: the intersection between signaling pathways involved in axon myelination and the inhibition of axon regeneration, *Front. Mol. Neurosci.*, 2016, vol. 9, art. ID 33. https://doi.org/10.3389/fnmol.2016.00033

Sachdeva, R., Gao, F., Chan, C.C.H., and Krassioukov, A.V., Cognitive function after spinal cord injury: a systematic review, *Neurology*, 2018, vol. 91, no. 13, pp. 611–621. https://doi.org/10.1212/WNL.0000000000006244

Schuh, C.M., Morton, T.J., Banerjee, A., et al., Activation of Schwann cell-like cells on aligned fibrinpoly (lactic-co-glycolic acid) structures: a novel construct for application in peripheral nerve regeneration, *Cells Tissues Organs*, 2015, vol. 200, no. 5, pp. 287–299. https://doi.org/10.1159/000437091

Shah, M., Peterson, C., and Yilmaz, E., Current advancements in the management of spinal cord injury: a comprehensive review of literature, *Surg. Neurol. Int.*, 2020, vol. 11, art. ID. 2. https://doi.org/10.25259/SNI_568_2019

Singh, A., Tetreault, L., Kalsi-Ryan, S., et al., Global prevalence and incidence of traumatic spinal cord injury, *Clin. Epidemiol.*, 2014, vol. 23, no. 6, pp. 309–331. https://doi.org/10.2147/CLEP.S68889

Steeves, J.D., Bench to bedside: challenges of clinical translation, *Prog. Brain Res.*, 2015, vol. 218, pp. 227–239. https://doi.org/10.1016/bs.pbr.2014.12.008

Swieck, K., Conta-Steencken, A., Middleton, F.A., et al., Effect of lesion proximity on the regenerative response of long descending propriospinal neurons after spinal transection injury, *BMC Neurosci.*, 2019, vol. 20, no. 1, art. ID 10. https://doi.org/10.1186/s12868-019-0491-y

Tatullo, M., Marrelli, M., Cassetta, M., et al., Platelet rich fibrin (P.R.F.) in reconstructive surgery of atrophied maxillary bones: Clinical and histological evaluations, *Int. J. Med. Sci.*, 2012, vol. 9, pp. 872–880. https://doi.org/10.7150/ijms.5119

Tran, A.P., Warren, P.M., Silver, J., et al., The biology of regeneration failure and success after spinal cord injury, *Physiol. Rev.*, 2018, vol. 98, no. 2, pp. 881–917. https://doi.org/10.1152/physrev.00017.2017

Wan, F.J., Chien, W.C., Chung, C.H., et al., Association between traumatic spinal cord injury and affective and other psychiatric disorders – A nationwide cohort study and effects of rehabilitation therapies, *J. Affective Disord.*, 2020, vol. 265, vol. 381–388. https://doi.org/10.1016/j.jad.2020.01.063

Wang, Y., Tan, H., and Hui, X., Biomaterial scaffolds in regenerative therapy of the central nervous system, *Biomed. Res. Int.*, 2018, vol. 2018, art. ID 784890.1 https://doi.org/10.1155/2018/7848901

Webb, A.A. and Muir, G.D., Compensatory locomotor adjustments of rats with cervical or thoracic spinal cord hemisections, *J. Neurotrauma*, 2002, vol. 19, no. 2, vol. 239–256. https://doi.org/10.1089/08977150252806983

Yao, S., Liu, X., Yu, S., et al., Co-effects of matrix low elasticity and aligned topography on stem cell neurogenic differentiation and rapid neurite outgrowth, *Nanoscale*, 2016, vol. 8, no. 19, pp. 10252–10265. https://doi.org/10.1039/c6nr01169a

Zhang, Q., Shi, B., and Ding, J., Polymer scaffolds facilitate spinal cord injury repair, *Acta Biomater.*, 2019, vol. 88, pp. 57–77. https://doi.org/10.1016/j.actbio.2019.01.056

Zhang, Q., Yan, S., You, R., et al., Multichannel silk protein/laminin grafts for spinal cord injury repair, *J. Biomed. Mater. Res., Part A*, 2016, vol. 104, no. 12, pp. 3045–3057. https://doi.org/10.1002/jbm.a.35851

Zhao, Y.Y., Yuan, Y., Chen, Y., et al., Histamine promotes locomotion recovery after spinal cord hemisection *via* inhibiting astrocytic scar formation, *CNS Neurosci. Ther.*, 2015, vol. 21, no. 5, pp. 454–462. https://doi.org/10.1111/cns.12379

Translated by N. Tarasyuk